ORIGINAL ARTICLE

Molecular Plant Pathology WILEY

Orchestration of virulence factor expression and modulation of biofilm dispersal in *Erwinia amylovora* through activation of the Hfq-dependent small RNA RprA

Jingyu Peng | Jeffrey K. Schachterle | George W. Sundin 🆔

Department of Plant, Soil, and Microbial Sciences, Michigan State University, East Lansing, Michigan, USA

Correspondence
George W. Sundin, Department of Plant, Soil, and Microbial Sciences, Michigan State University, East Lansing, Michigan, USA.
Email: sundin@msu.edu

Present address
Jeffrey K. Schachterle, US National Arboretum – Floral and Nursery Plants Research Unit, USDA-ARS, Beltsville, Maryland, USA

Abstract

Erwinia amylovora is the causative agent of the devastating disease fire blight of pome fruit trees. After infection of host plant leaves at apple shoot tips, *E. amylovora* cells form biofilms in xylem vessels, restrict water flow, and cause wilting symptoms. Although *E. amylovora* is well known to be able to cause systemic infection, how biofilm cells of *E. amylovora* transit from the sessile mode of growth in xylem to the planktonic mode of growth in cortical parenchyma remains unknown. Increasing evidence has suggested the important modulatory roles of Hfq-dependent small RNAs (sRNAs) in the pathogenesis of *E. amylovora*. Here, we demonstrate that the sRNA RprA acts as a positive regulator of amylovoran exopolysaccharide production, the type III secretion system (T3SS), and flagellar-dependent motility, and as a negative regulator of levansucrase activity and cellulose production. We also show that RprA affects the promoter activity of multiple virulence factor genes and regulates *hrpS*, a critical T3SS regulator, at the posttranscriptional level. We determined that *rprA* expression can be activated by the Rcs phosphorelay, and that expression is active during T3SS-mediated host infection in an immature pear fruit infection model. We further showed that overexpression of *rprA* activated the in vitro dispersal of *E. amylovora* cells from biofilms. Thus, our investigation of the varied role of RprA in affecting *E. amylovora* virulence provides important insights into the functions of this sRNA in biofilm control and systemic infection.

KEYWORDS
biofilm dispersal, fire blight, posttranscriptional regulation, small RNA, systemic infection

1 | INTRODUCTION

Fire blight, caused by *Erwinia amylovora*, is a devastating bacterial disease threatening the worldwide production of many rosaceous fruits, such as apple and pear (Malnoy et al., 2012). The primary infection of

E. amylovora is manifested by several distinct stages: flower infection, infection of leaves at shoot tips, xylem colonization, and systemic infection. During flower infection, large populations of *E. amylovora* cells (c.10^{6-7} cfu/flower) are established on stigmas; these bacteria are then further disseminated down to the hypanthium, and ultimately initiate

infection via natural openings in the flower nectaries (Thomson, 2000; Vanneste, 1995). Within host xylem vessels in leaves, *E. amylovora* cells block water transport and cause wilting symptoms by formation of biofilms, which are static microcolonies of bacterial cells enmeshed in a matrix of exopolysaccharides (EPSs) (Castiblanco & Sundin, 2016; Kharadi & Sundin, 2020; Koczan et al., 2009, 2011; Mina et al., 2019). *E. amylovora* cells can migrate further within the vascular tissue to cause systemic infection, but more commonly exit from xylem vessels and move further systemically through the host in cortical parenchyma tissue. The systemic spread of *E. amylovora* through host apple trees follows a downward path, ultimately ending at the crown–rootstock junction, where cankers can develop that girdle and kill the host (Norelli et al., 2003). Frequently, *E. amylovora* cells emerge from flower pedicel, leaf petiole, or stem tissues as ooze, which serves as the inoculum for secondary infection (Slack et al., 2017).

The pathogenesis of *E. amylovora* is mediated by several important virulence factors, including the type III secretion system (T3SS) (Oh et al., 2005; Zhao et al., 2009a), motility (Bayot & Ries, 1986), and several EPSs including amylovoran (Goodman et al., 1974; Sjulin & Beer, 1978), levan (Geier & Geider, 1993), and cellulose (Castiblanco & Sundin, 2018). The primary infection of *E. amylovora* through flowers requires motility to facilitate the migration of *E. amylovora* cells from stigmas to nectarthodes, and the T3SS to defeat host defence mechanisms and initiate pathogenesis (Bayot & Ries, 1986; Bogdanove et al., 1998; Kim et al., 1997; Oh et al., 2005). The T3SS is major pathogenicity factor of *E. amylovora* that has been well characterized to be regulated in a hierarchical manner. HrpL, an alternate sigma factor, activates transcription of the *hrp* genes, including the structural gene *hrpA* encoding the T3SS pilus, and the major effector gene *dspE*, through recognition of the "hrp box" motif (McNally et al., 2012; Triplett et al., 2009; Wei & Beer, 1995). *hrpL* expression is tightly regulated by the enhancer-binding protein HrpS and the two-component system HrpX/HrpY (Lee et al., 2016; Wei et al., 2000). Amylovoran, an acidic exopolysaccharide composed of repeating units of galactose molecules and a glucuronic acid residue, is another main pathogenicity factor of *E. amylovora* (Bellemann & Geider, 1992; Nimtz et al., 1996). Amylovoran biosynthesis is mediated by the 12-gene *ams* operon (Bugert & Geider, 1995). Levan is a homopolymer of fructose molecules synthesized through hydrolysis of sucrose via the levansucrase enzyme that is encoded by the *lsc* gene (Geier & Geider, 1993; Gross et al., 1992). Amylovoran, levan, and cellulose together constitute the matrix of *E. amylovora* biofilms (Castiblanco & Sundin, 2018; Koczan et al., 2009).

The chaperone protein Hfq functions to stabilize its dependent small RNAs (sRNAs) and to facilitate the interactions of these sRNAs with their mRNA targets (Brennan & Link, 2007). Hfq-dependent sRNA–mRNA interactions result in posttranscriptional regulation through either activation or inhibition of translation (Vogel & Luisi, 2011). Hfq and its associated sRNAs play critical roles in the regulation of pathogenesis in gram-negative plant pathogenic bacteria such as *Agrobacterium tumefaciens*, *Burkholderia glumae*, *Dickeya dadantii*, *E. amylovora*, *Pantoea ananatis*, *Pectobacterium carotovorum*, and *Xanthomonas campestris* (Kim et al., 2018; Lai et al., 2018; Wang et al., 2018; Wilms et al., 2012; Yuan et al., 2019; Zeng et al., 2013;

Zeng & Sundin, 2014). In *E. amylovora*, the Hfq-dependent sRNA ArcZ was shown to positively affect amylovoran biosynthesis, the T3SS, levansucrase activity, and flagellar swimming motility, partially through posttranscriptional regulation of the leucine-responsive regulatory protein Lrp (Schachterle & Sundin, 2019; Schachterle et al., 2019; Zeng & Sundin, 2014). However, the functions and regulatory mechanisms of most Hfq-dependent sRNAs identified in *E. amylovora* are still enigmatic. A deletion mutant of the Hfq-dependent sRNA *rprA* (Ea1189∆*rprA*) was previously shown to cause decreased levels of virulence in an immature pear infection model, suggesting the positive involvement of this sRNA in the pathogenesis of *E. amylovora* through unknown mechanisms (Zeng et al., 2013). RprA was initially identified in *Escherichia coli*, and was shown to stimulate the translation of the stationary-phase sigma factor RpoS in this bacterium (Majdalani et al., 2001). Through imperfect reverse complementarity with RprA, the inhibitory structure of the 5′ untranslated region (5′ UTR) of the *rpoS* mRNA is disengaged and the translation of *rpoS* is consequently activated (Majdalani et al., 2001; McCullen et al., 2010; Urban & Vogel, 2007). *E. coli* RprA has also been shown to down-regulate *csgD*, encoding a stationary phase-induced biofilm regulator, and *ydaM*, encoding a diguanylate cyclase (Andreassen et al., 2018; Mika et al., 2012). Expression of *E. coli* RprA has been demonstrated to be induced by the RcsCDB phosphorelay (Majdalani et al., 2002). On stimulation, the hybrid sensor kinase RcsC transfers a phosphoryl group to RcsD and then to the response regulator RcsB (Huang et al., 2006). The phosphorylated RcsB further modulates the expression of the downstream genes through binding to the "Rcs box" in promoter regions (Ancona et al., 2015; Huang et al., 2006; Wang et al., 2009). RprA expression in *E. coli* or *Salmonella enterica* serovar Typhimurium can also be activated by high population density and by environmental stressors, including osmolarity shock and low pH (Madhugiri et al., 2010; Srikumar et al., 2015).
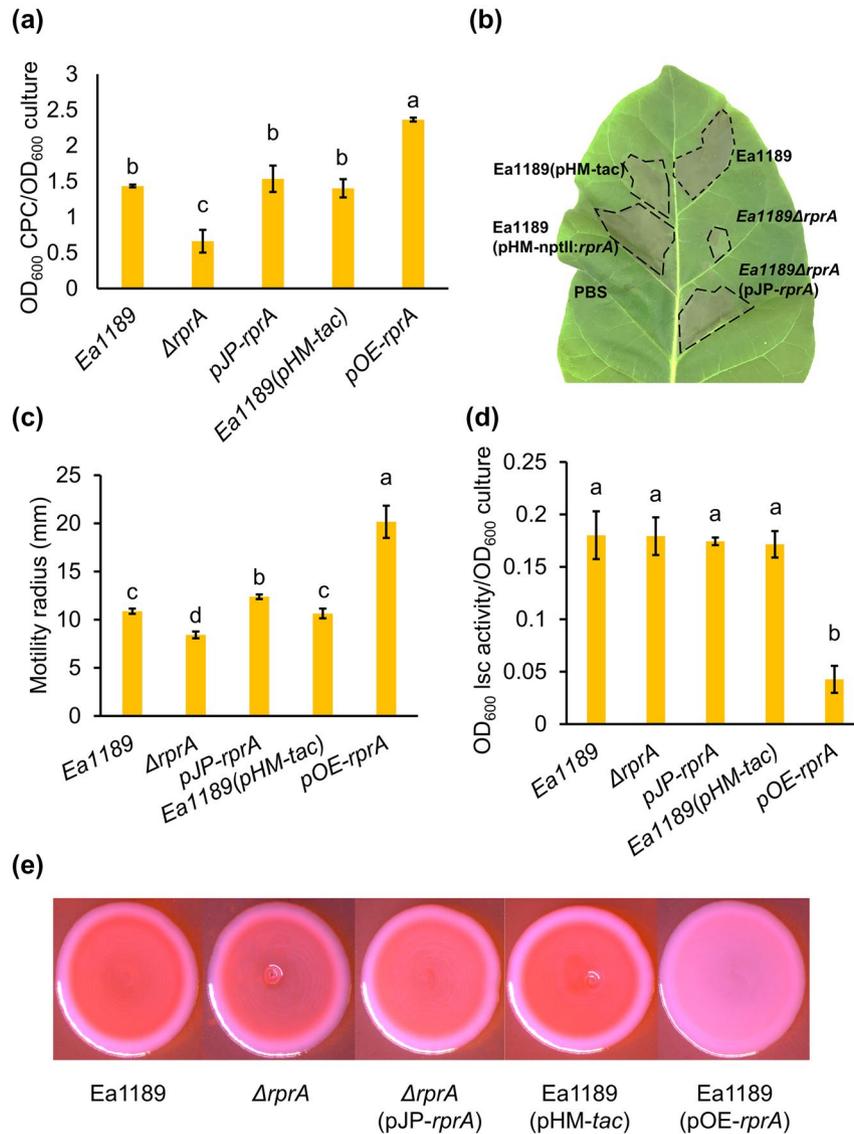
We hypothesized that RprA affects the virulence of *E. amylovora* through modulation of its virulence factor(s), and that expression of *rprA* is activated or deactivated during *E. amylovora* pathogenesis upon perception of certain environmental cues. In this study, we demonstrate that RprA acts as a positive regulator of amylovoran, T3SS, and flagellar-dependent motility, and as a negative regulator of levansucrase activity and cellulose production. We also identified the in vitro and in vivo conditions that activate RprA and demonstrated that activation of RprA decreased biofilm formation and promoted biofilm dispersal. This study provides important evidence for the involvement of RprA in the systemic movement of *E. amylovora* during pathogenesis.

2 | RESULTS

2.1 | RprA positively regulates amylovoran, T3SS, and motility, and negatively regulates levansucrase activity and cellulose production

RprA was previously identified as a 111-nucleotide Hfq-dependent sRNA that contributed to the full virulence of *E. amylovora*, as the

deletion mutant Ea1189Δ*rprA* showed compromised virulence in an immature pear infection model (Zeng et al., 2013). To validate the positive involvement of RprA in the virulence of *E. amylovora*, we first examined the virulence of Ea1189Δ*rprA* (pJP-*rprA*), in which *rprA* was expressed in trans. We showed that Ea1189Δ*rprA* (pJP-*rprA*) exhibited strong virulence on the inoculated immature pears that was comparable to the *E. amylovora* wild-type (WT) strain (Figure 1a), confirming the importance of RprA on the virulence of *E. amylovora*. Secondary structure modelling of RprA showed that RprA had four stem-loops with a characteristic rho-independent terminator in the 3′ end (Figure 1b). Sequence alignment of the RprA homologs in the *Enterobacteriaceae* family suggested that nucleotide sequences of RprA are highly conserved towards the 3′ end but much less conserved towards the 5′ end (Figure 1c).

To understand the molecular mechanisms of RprA in affecting the full virulence of *E. amylovora*, we examined how mutagenesis or overexpression of *rprA* affected virulence factors of this bacterium, including amylovoran production, hypersensitive response (HR), flagellar swimming motility, levansucrase activity, and cellulose production. We showed that amylovoran production was significantly reduced in the Ea1189Δ*rprA* mutant, and that production was restored to the WT level in the complementation strain (Figure 2a). In contrast, overproduction of RprA rendered a significantly increased level of amylovoran production in *E. amylovora* (Figure 2a). Our results therefore suggested that RprA is a positive regulator of amylovoran production. To investigate if RprA affected the function of T3SS, we examined whether deletion of *rprA* or overproduction affected the ability of *E. amylovora* to elicit the HR. Compared with

(a) Ea1189 Δ*rprA* Δ*rprA*(pJP-*rprA*) Δ*ams*

(b)

(c)

Citrobacter rodentium	AACGUUAUAAAUCAACACAUUGAUUU---AUAAGCA--UGGAAAUCCCCUGAGUGAAACA
Salmonella enterica	ACGGUUAUAAAUCAACACAUUGAUUU---AUAAGCA--UGGAAAUCCCCUGAGUGAAACA
Escherichia coli	ACGGUUAUAAAUCAACAUAUUGAUUU---AUAAGCA--UGGAAAUCCCCUGAGUGAAACA
Escherichia fergusonii	ACGGUUAUAAAUCAACGUAUUGAUUU---AUAAGCA--UGGAAAUCCCCUGAGUGAAACA
Citrobacter koseri	ACGGUUAUAAAUCAACGCCUUGAUUU---AUAAGCA--UGGAAAUCCCCUGAGUGAAACA
Klebsiella pneumoniae	ACGGUUAUAAAUCAACACCUUGAUUU---AUAAGCA--UGGAAAUCCCCUGAGUGAAACA
Erwinia amylovora	AGGAUUUGAAAUCUUCCCACUGAUUUUGAAUUAACAGACUUACCCCCCUGAGUUAACUA
Erwinia pyrifoliae	AAGUUUUGAAAUCUACCCACUGAUUUUGAAUUAACAGACUUA---CCCCUGAGUUAACUA
Erwinia billingiae	CAUGUUUAUGAUCAAACCGCUGAUUU---CUAAACA-ACCUUUUUCCCCUGAGUAAACUA
Pantoea stewartii	CAAGUUUGAAAUCAACUCACUGAUUU---CUAAACCCCUUAUUUCCCCUGAGUAGCGUA
	** *** ****** * * ** ******** *

Citrobacter rodentium	ACGAAUUGCUGUGUGUAGUCUUUGCCCAUCUCCCACGAUGGGCUUUUUUU-
Salmonella enterica	ACGAAUUGCUGUGUGUAGUCUUUGCCCGUCUCCUACGAUGGGCUUUUUUU-
Escherichia coli	ACGAAUUGCUGUGUGUAGUCUUUGCCCAUCUCCCACGAUGGGCUUUUUUU-
Escherichia fergusonii	ACGAAUUGCUGUGUGUAGUCUUUGCCCAUCUCCCACGAUGGGCUUUUUUU-
Citrobacter koseri	ACGAAUUGCUGUGUGUAGUCUUUGCCCAUCUCCCACGAUGGGCCUUUUUU-
Klebsiella pneumoniae	ACGAAUUGCUGUGUGUAGUCUUUGCCCAUCUCCCACGAUGGGCUUUUUUUU
Erwinia amylovora	AAGAAUUGCUGUGUGUAGUCUUUGCCCAUCCCCUGUGAUGGGCUUUUUUUU
Erwinia pyrifoliae	AAGAAUUGCUGUGUGUAGUCUUUGCCCAUCCACUGUGAUGGGCUUUUUUUU
Erwinia billingiae	AAGAAUUGCUGUGUGUAGUCUUUGCCCAUCCCAUGUGAUGGGCUUUUUUUU
Pantoea stewartii	AAGAAUUGCUGUGUGUAGUCUUUGCCCACCCCCCUGUGAUGGGCUUUUUUUU
	* ************************ * ******* ******

FIGURE 1 The effect of *RprA* on virulence of *Erwinia amylovora* and sequence characteristics of RprA. (a) *E. amylovora* strains at approximately 2×10^4 cfu in 2 μl were stab-inoculated into immature pears. Images were captured 4 days postinoculation. The amylovoran-null mutant Ea1189Δ*ams* was used as a negative control for the assays. (b) Secondary structure of RprA was predicted with the minimum free energy model of RNAfold (http://rna.tbi.univie.ac.at/cgi-bin/RNAWebSuite/RNAfold.cgi). The positional entropy of each nucleotide is colour-coded. (c) Sequence alignment of RprA homologs in representative species of *Enterobacteriaceae*. Shared nucleotide sequences are highlighted in green

FIGURE 2 Multifaced regulatory roles of RprA on virulence factors of *Erwinia amylovora*. (a) RprA positively regulates amylovoran production. Amylovoran was determined in cultures grown for 24 hr in MBMA medium with 1% galactose using a cetylpyridinium chloride-binding assay. (b) Positive involvement of RprA in affecting the hypersensitive response (HR) elicited by *E. amylovora*. Approximately 100 μl cell suspension at $OD_{600} = 0.05$ was infiltrated into leaves of 10-week-old *Nicotiana benthamiana* plants. The HR was observed 16 hr postinoculation. (c) RprA increases the swimming motility of *E. amylovora*. Overnight cultures (2 μl) were inoculated into 0.3% agar LB plates, and the radius of the motility area was measured after 48 hr. (d) RprA inhibits levansucrase (Lsc) activity of *E. amylovora*; Lsc activity was quantified as previously described (Schachterle & Sundin, 2019). (e) RprA inhibits cellulose biosynthesis in *E. amylovora* determined through a Congo red-binding assay. A greater amount of Congo red absorbance into the colony indicates an increased amount of cellulose production. For all of the in vitro assays, cultures were grown in the test media amended with 1 mM IPTG. Results represent the means of three biological replications and error bars represent the standard deviations. Different letters indicate significant differences ($p < .05$) using Tukey's HSD test. The assays were done at least three times with similar results

the other strains examined, the Ea1189Δ*rprA* mutant exhibited a minimal HR on *Nicotiana benthamiana* leaves, suggesting a positive effect of RprA on the function of T3SS (Figure 2b). The *rprA* mutation had a small effect on the swimming motility of *E. amylovora* (Figure 2c). In contrast, the *rprA* overexpression strain Ea1189(pOE-*rprA*) was hypermotile (Figure 2c). These results suggested that the basal level of RprA contributes little to the swimming motility of *E. amylovora*, but its effect on this phenotype was greater when *rprA* was overexpressed. Deletion mutation of *rprA* had negligible

effects on the activity of levansucrase and the production of cellulose, but these EPSs were greatly compromised when *rprA* was overexpressed (Figure 2d,e). Therefore, a basal level of RprA had minimal effects on levansucrase activity and cellulose production; a high level of RprA, nevertheless, negatively correlated with the production of these extracellular polymeric substances. Taken together, RprA exhibited complex regulatory roles on the virulence factors of *E. amylovora*, and these impacts were greater when RprA was overproduced.

2.2 | RprA regulates the promoter activity of virulence factor genes

To examine how RprA affected the transcriptional activity of virulence factor genes, we generated green fluorescent protein (gfp) transcriptional fusion reporter constructs of *amsG*, the first gene of the amylovoran biosynthetic gene operon, *lsc*, the levansucrase gene, and representative T3SS genes including *hrpL*, *hrpA*, and *dspE*. Compared with the empty vector strain, the *rprA* overexpression strain exhibited significantly higher promoter activity of *amsG* and of all of the T3SS genes examined (Figure 3). However, the promoter activity of *lsc* in the *rprA* overexpression strain was significantly lower; this was consistent with observation of reduced levansucrase activity in this strain compared with the control (Figure 3).

2.3 | RprA regulates *hrpS* at a posttranscriptional level

To identify possible direct targets of RprA, we conducted a genome-wide prediction of the targets of RprA using TargetRNA2 (Kery et al., 2014), which employs structural accessibility and sequence conservation for sRNA target screening. This analysis yielded prediction of 31 putative targets of RprA (Table S1). Of interest, the enhancer-binding protein gene *hrpS* was predicted as a target of RprA. RprA was predicted to interact with the region from −20 to −7 bp relative to the translational start site of *hrpS* (Figure 4a). Two transcriptional start sites of *hrpS* were previously identified at 129 and 227 nucleotides (nt) upstream from its start codon, respectively (Lee & Zhao, 2018). To determine whether RprA affected *hrpS* mRNA posttranscriptionally, we constructed pxg-20:*hrpS*129 and pxg-20:*hrpS*227,

which fused the 5′ untranslated region in 129 nt or 227 nt and the first 30 codons of *hrpS* in-frame with *gfp* in pXG-20. We found that overexpression of *rprA* resulted in significantly higher fluorescence in *E. amylovora* cells carrying pxg-20:*hrpS*129, but no significant difference was observed in cells carrying the pxg-20:*hrpS*227 construct (Figure 4b).

2.4 | *rprA* expression is activated by native and environmental cues

A previous study in *E. coli* showed that *rprA* was transcriptionally regulated by the Rcs phosphorelay, which is composed of the histidine kinase RcsC and the response regulator RcsB (Majdalani et al., 2002). We identified an "Rcs box," the consensus binding site of RcsB, immediately upstream of the −35 region of the promoter of *rprA* (Figure S1), suggesting that *rprA* in *E. amylovora* may also be subject to the regulation by the Rcs phosphorelay. As expected, compared with that in the WT strain, the expression of *rprA* was reduced approximately two-fold in the *rcsB* deletion mutant, Ea1189Δ*rcsB* (Figure 5a). Introduction of the complementation construct pJP-*rcsB* completely restored the *rprA* expression defect in Ea1189Δ*rcsB*, which was four-fold higher compared with the WT strain (Figure 5a). We also measured expression of *rprA* in Ea1189Δ*rcsB*(p*rcsB*-D56E) and Ea1189Δ*rcsB*(p*rcsB*-K154Q), which encoded RcsB with a D56E (aspartate to glutamic acid) substitution or a K154Q (lysine to glutamine) substitution to mimic the constitutively phosphorylated or the acetylated state of RcsB, respectively (Ancona et al., 2015; Hu et al., 2013). We showed that *rprA* expression was further elevated in Ea1189Δ*rcsB*(p*rcsB*-D56E) compared with Ea1189Δ*rcsB*(p*rcsB*), whereas its expression in Ea1189Δ*rcsB*(p*rcsB*-K154Q) was reduced
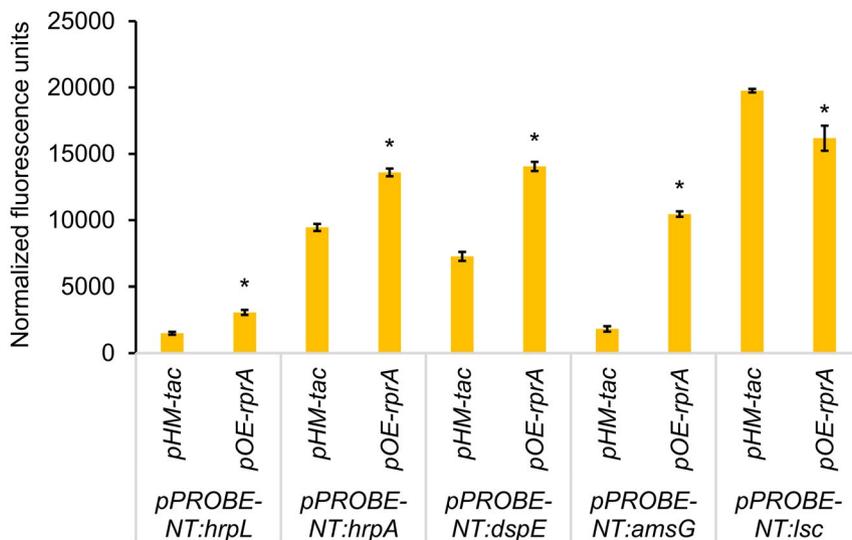
FIGURE 3 RprA regulates the promoter activity of *Erwinia amylovora* virulence factor genes. Relative fluorescence units of the indicated transcriptional fusion construct in Ea1189(pHM-*tac*) and Ea1189(pOE-*rprA*) were measured using a Tecan spectrophotometer followed by normalization with the corresponding OD$_{600}$ values. IPTG at 1 mM was amended into the medium to induce *rprA* overexpression. Results represent the means of three biological replications and error bars represent the standard deviation of the means. Asterisks indicate significant difference ($p < .05$) using Student's *t* test. The assays were done three times with similar results

(a)

(b)
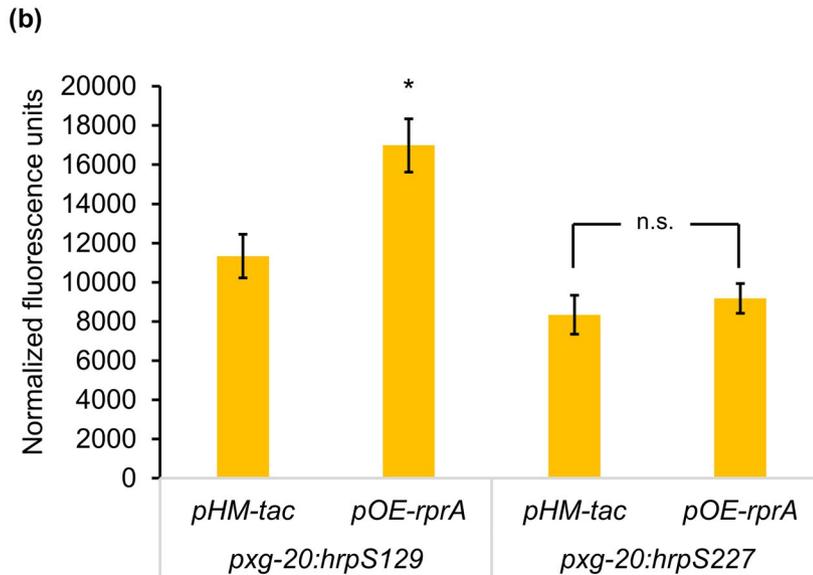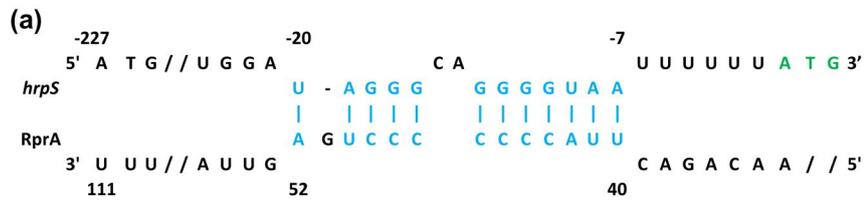
FIGURE 4 RprA regulates *hrpS* at the posttranscriptional level. (a) Proposed interaction region between RprA and *hrpS* mRNA. (b) Relative fluorescence units of the indicated translational fusion in Ea1189(pHM-*tac*) and Ea1189(pOE-*rprA*) were measured using a Tecan spectrophotometer followed by normalization of their corresponding OD_{600} values. Results represent the means of three biological replications and error bars represent the standard deviations. Asterisks indicate significant difference ($p < .05$), whereas n.s. indicates no significant difference using Student's *t* test. The assays were done three times with similar results

(a)

(b)
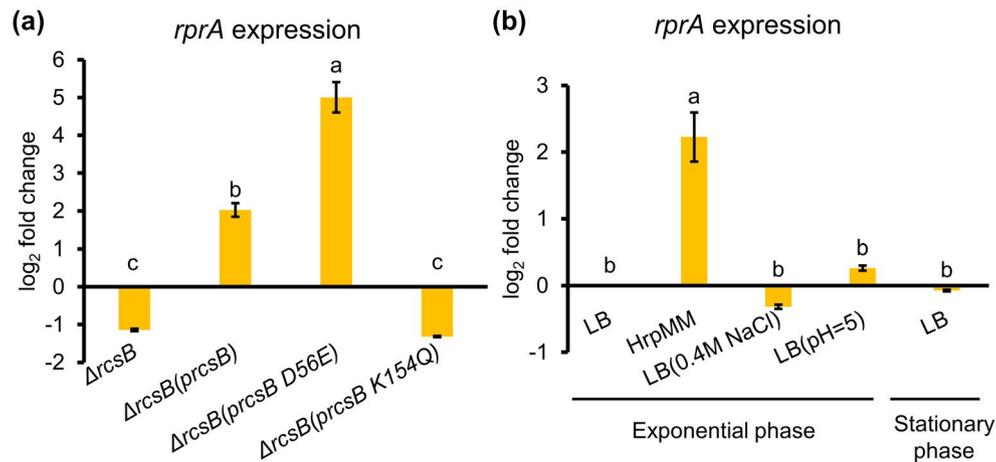
FIGURE 5 Activation of RprA by native and environmental cues. (a) Regulation of RprA expression by the Rcs phosphorelay system. (b) Effect of environmental stressors on *rprA* expression. Expression levels of *rprA* were quantified using quantitative reverse transcription PCR (RT-qPCR), and fold changes were calculated using the $2^{-\Delta\Delta Ct}$ formula. The housekeeping gene *recA* was used as an endogenous control. Error bars indicate standard deviations of the means. Different letters indicate significant differences ($p < .05$) using Tukey's HSD test

to a level comparable to that of Ea1189Δ*rcsB* (Figure 5a). Together, these results indicate that *rprA* expression is positively and negatively modulated by the phosphorylation and the acetylation of RcsB, respectively.

To examine whether expression of *rprA* could be affected by external stressors, *E. amylovora* Ea1189 WT cultures were grown in Luria Bertani (LB) broth to exponential phase ($OD_{600} = 0.5$) and then challenged with either low pH (pH 5) or osmotic shock (0.4 M

NaCl), or immersed in HrpMM medium, a low pH and low nutrient medium that mimics the conditions of the plant apoplast (Huynh et al., 1989). We also examined how the population density of *E. amylovora* (exponential phase versus stationary phase) may affect *rprA* expression. We did not observe any significant change of *rprA* expression in *E. amylovora* cells undergoing low pH stress or osmotic shock or in high population density (Figure 5b). However, *rprA* expression was significantly induced in *E. amylovora* cultures grown in

HrpMM (Figure 5b), suggesting that *rprA* may be induced during host infection.

To enable in vivo examination of *rprA* transcriptional activity, we generated the dual reporter construct p*NptII-gfp-rprA-mCherry*, which allowed cellular *gfp* expression in a constitutive manner and mCherry under the control of the native promoter of *rprA*. As observed using a confocal microscope, the transcriptional activity of *rprA* was very low in Ea1189(p*NptII-gfp-rprA-mCherry*) cultures grown in LB broth (Figure 6a), as indicated by the very dim fluorescence from mCherry. In immature pear flesh tissue that was inoculated with Ea1189(p*NptII-gfp-rprA-mCherry*), *E. amylovora* cells were shown to colonize the apoplast region of the flesh tissue (green fluorescence) and also exhibited strong levels of red fluorescence (Figure 6a). In pear ooze that contained a large population of *E. amylovora* cells emerging from the infection site of the inoculated pears, *E. amylovora* cells also exhibited very high levels of red fluorescence compared with that in LB broth. Through quantitative reverse transcription PCR (RT-qPCR), we confirmed that *rprA* expression increased by c.30-fold in *E. amylovora* cells from pear ooze compared with that grown in LB broth (Figure 6b). We also showed

up-regulation of the T3SS genes and the amylovoran biosynthetic gene *amsG*, and down-regulation of the levansucrase gene *lsc* in *E. amylovora* cells from pear ooze (Figure 6b). Taken together, our results showed that *rprA* expression was activated in vitro by conditions mimicking the plant apoplast environment or in vivo during host infection.

2.5 | *rprA* inhibits biofilm formation and activates dispersal of biofilm cells

RprA activation induced amylovoran production, which promotes formation of biofilms; activation of RprA also induced flagellar-dependent motility and inhibited production of levan and cellulose, which promotes dispersal of biofilm cells. To resolve this paradox, we examined the total effects of RprA on formation and dispersal of biofilm cells. We quantified biofilm formation in isopropyl-β-D-1-thiogalactopyranoside (IPTG)-supplemented cultures of Ea1189(pHM-*tac*) and Ea1189(pOE-*rprA*) through a microtitre plate assay. Compared with the empty vector control, Ea1189(pOE-*rprA*)

(a)

FIGURE 6 In vivo activation of RprA during host infection. (a) Confocal observation of *rprA* promoter activity in *Erwinia amylovora* Ea1189(p*NptII-gfp-rprA-mCherry*) in LB medium and in flesh and ooze of inoculated immature pears. Gfp (ex/em = 488 nm/510 nm) is expressed constitutively, whereas mCherry (ex/em = 587 nm/610 nm) is expressed under the control of the promoter of *rprA* in Ea1189(p*NptII-gfp-rprA-mCherry*) cultures. Images were captured through sequential scanning using a FluoView 1000 (Olympus) laser scanning confocal microscope. (b) Expression of *rprA* and several virulence factor genes in *E. amylovora* Ea1189 cells emerged in ooze from the inoculated immature pears and from cells that were grown overnight in LB medium. To ensure representativity of gene expression levels in *E. amylovora* cells from pear ooze, ooze from groups of six of the 18 inoculated pears were pooled together as one biological replication (labelled as "Ooze 1", "Ooze 2", and "Ooze 3"). Gene expression levels were quantified through quantitative reverse transcriptionPCR and fold changes were calculated using the $2^{-\Delta\Delta Ct}$ formula. The housekeeping gene *recA* was used as an endogenous control. Error bars indicate standard deviations of the mean within each biological replication

(b)
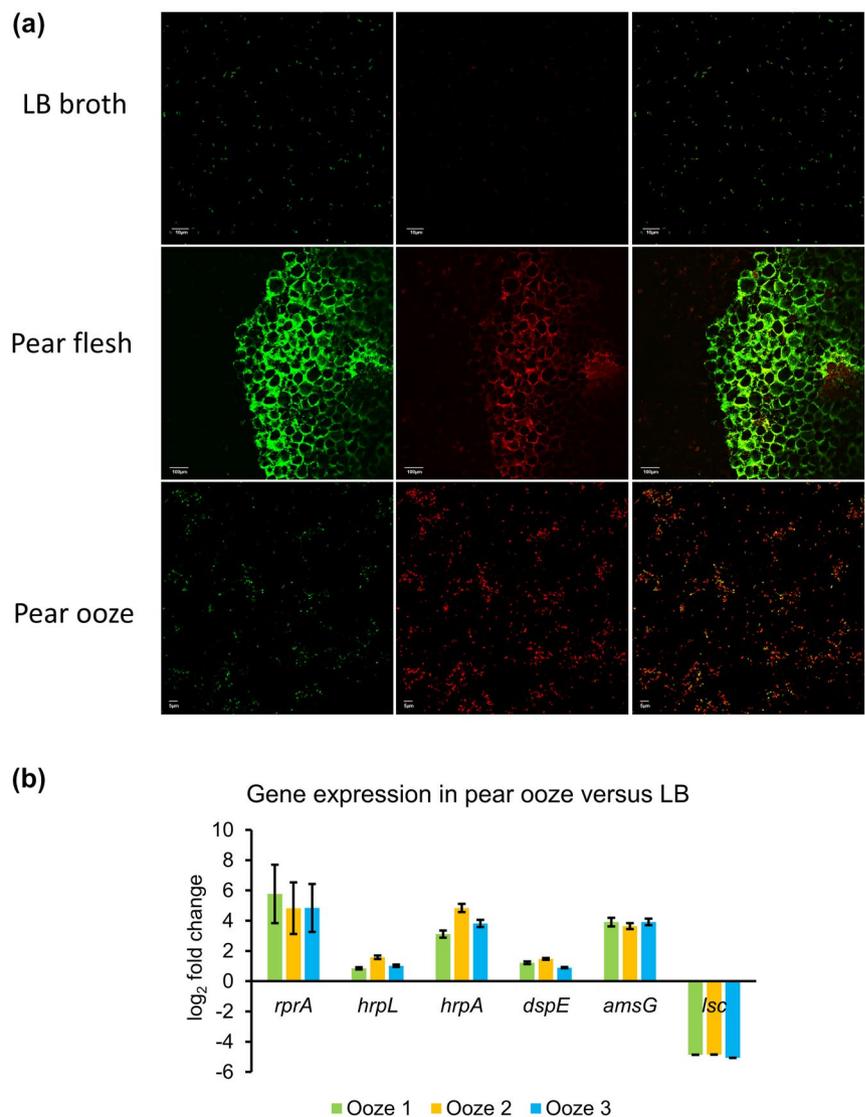
cultures formed significantly less biofilm, suggesting an overall negative effect of RprA on biofilm formation (Figure 7a). We then questioned how induction of *rprA* affects biofilm dispersal. To investigate this, we first let strains of Ea1189(pHM-*tac*) or Ea1189(pOE-*rprA*) form biofilms on polystyrene beads without addition of any IPTG into the medium. Washed beads covered with biofilms were then transferred to fresh medium containing 1 mM IPTG. Cells that dispersed into the medium were periodically quantified through dilution plating. We showed that overexpression of *rprA* did not affect the number of dispersed cells in the first hour after induction (Figure 7b). However, significantly more cells of Ea1189(pOE-*rprA*) were dispersed in the IPTG induction condition compared with Ea1189(pHM-*tac*) from 2 to 5 hr after IPTG addition, and the differences were greater as the experiments continued (Figure 7b). These

FIGURE 7 RprA negatively affects biofilm formation and activates biofilm dispersal in vitro. (a) Biofilm formation of *Erwinia amylovora* Ea1189(pHM-*tac*) and Ea1189(pOE-*rprA*) cultures. Cultures at $OD_{600} = 1.0$ were resuspended in $0.5 \times LB$ medium containing 1 mM IPTG and were inoculated into acetone-etched microtitre plates for 48 hr. Biofilms were quantified through a crystal violet (CV) staining assay at the absorbance of 594 nm (A_{594}). (b) Temporal dispersal of biofilm cells. Polystyrene beads (7 mm) were immersed into *E. amylovora* cultures in $0.5 \times LB$ medium without any IPTG for 48 hr. Beads covered by biofilm were washed and dipped into fresh $0.5 \times LB$ medium with 1 mM IPTG. Planktonic cultures were periodically withdrawn, and cfus were determined using dilution plating (line graph). To count the number of cells covered on the beads before and after dispersal, biofilm-covered beads were immersed into $0.5 \times$ phosphate-buffered saline and were sonicated for 5 min to release the attached cells for cell count through dilution plating (bar graph). The assays were done three times with similar results

results indicated that induction of *rprA* negatively impacts biofilm formation and positively impacts dispersal of *E. amylovora* cells from biofilms. A working model for the functions of RprA is proposed (Figure 8).

3 | DISCUSSION

Our results demonstrate that the Hfq-dependent sRNA RprA regulates a varied group of virulence factors of *E. amylovora* that impact pathogenesis and systemic movement through the apple host. The regulatory impact of RprA on virulence would seem to mostly occur via direct interactions with mRNAs of transcriptional regulators of the associated virulence factor. For example, we demonstrated that RprA activates *hrpS* mRNA at a posttranscriptional level, probably via a direct interaction with *hrpS* mRNA. As the enhancer-binding protein HrpS functions to activate the transcription of *hrpL*, encoding the alternative sigma factor HrpL, which is required for the transcription of all other genes within the Hrp regulon, the translational stimulation of *hrpS* due to *rprA* overexpression therefore explained its positive effects on the promoter activity of the downstream T3SS genes, including *hrpL*, *hrpA*, and *dspE*. Of note, RprA appeared to only affect the 129-nt 5′ UTR but not the 227-nt 5′ UTR of *hrpS*, suggesting that the longer 5′ UTR of *hrpS* forms a distinct structure that is inaccessible to RprA and may or may not require an additional but yet unidentified factor(s) to regulate its translation.

We also found that RprA is a positive regulator of amylovoran production through a positive effect on the promoter of *amsG*, the first gene of the amylovoran biosynthetic gene operon, and also has a negative effect on the expression of the levansucrase gene *lsc*. Transcriptional regulation of the 12-gene *ams* operon, encoding amylovoran biosynthesis, is highly complex. This probably occurs for many reasons, including that the amylovoran EPS is required for pathogenicity (Norelli et al., 2003) and is the most important EPS component of *E. amylovora* biofilms (Koczan et al., 2009), and also reflects the inverse regulation of biofilm formation and expression of the T3SS (Edmunds et al., 2013). Positive transcriptional regulators of the *ams* operon include the Rcs phosphorelay via direct interaction with an Rcs box (Wang et al., 2009, 2012b; Zhao et al., 2009b); *ams* operon expression is also positively regulated by the second messenger molecule cyclic di-GMP via an as yet unknown transcriptional regulator (Edmunds et al., 2013). Negative transcriptional regulators of the *ams* operon include the EnvZ/OmpR and GrrA/GrrS two-component systems (Zhao et al., 2009b), and AmyR, a member of the enterobacterial YbjN family (Wang et al., 2012a). Thus, there are many potential targets that RprA might interact with to positively impact transcription of the *ams* operon.

It is noteworthy that we determined most functions of RprA from the overexpression studies but not from the mutagenesis studies. Compared with the WT strain, the Ea1189Δ*rprA* mutant had negligible effects on swimming motility, levansucrase activity, and cellulose production. This suggests that the basal level of RprA in *E. amylovora* cells grown in a rich medium is too low to have

FIGURE 8 Proposed model of the functions of the Hfq-dependent sRNA RprA in modulating virulence factors and systemic infection of *Erwinia amylovora*. After infection of leaves at shoot tips, *E. amylovora* cells form biofilms within xylem vessels of the host plants. Expression of *rprA* is activated in *E. amylovora* cells upon perception of environmental cues, including RcsB phosphorylation and the host apoplast environment. Through regulation of virulence factor genes at the transcriptional (plain font) or posttranscriptional (bold font) level, RprA positively regulates amylovoran exopolysaccharide and the type III secretion system (T3SS), the two major pathogenicity factors of *E. amylovora*, and flagellar-dependent motility, which has a known negative correlation with biofilm formation in *E. amylovora*; RprA also negatively affects production of levan and cellulose, which are constituents of the matrix of *E. amylovora* biofilms. The total effects of RprA promote the transition of biofilm cells of *E. amylovora* in the sessile mode of growth within host xylem tissue to the planktonic mode of growth; this consequently facilitates the further systemic infection of *E. amylovora* cells within the vascular or the cortical parenchyma tissue of host plants

strong effects on the measured phenotypes. Indeed, the promoter activity of *rprA* was very low in *E. amylovora* cells grown in LB medium, as indicated by the dim red fluorescence using the dual reporter system. These observations are reminiscent of previous studies of RprA in *E. coli*. Through assays of an *rprA-lacZ* fusion or northern blot, several studies have shown that *rprA* is nearly undetectable in WT *E. coli* cells grown in a rich medium (Madhugiri et al., 2010; Majdalani et al., 2001, 2005). In line with this, known targets of RprA in *E. coli*, including *rpoS*, *csgD*, and *ydaM*, were consistently identified through overexpression of this sRNA, whereas a *rprA* knockout mutation hardly affected any of these targets (Majdalani et al., 2002; Mika et al., 2012). Therefore, a basal level of RprA in the bacteria grown in a rich medium functions minimally in affecting its targets, which are nevertheless strongly perturbed by overproduction of this sRNA.

We demonstrated that *rprA* expression was under the tight regulation of the Rcs phosphorelay, as *rprA* expression was reduced by about one half in the Ea1189Δ*rcsB* mutant compared with the WT Ea1189 strain. A similar level of decrease of the transcriptional activity of *rprA* in *E. coli* was previously reported in a corresponding Δ*rcsB* mutant (Majdalani et al., 2002). In *E. coli*, *rprA* was shown to be positively regulated by RcsB when the protein was phosphorylated, and negatively regulated by RcsB when the protein was acetylated (Hu et al., 2013; Majdalani et al., 2002; Szczesny et al., 2018), which is consistent with our observation of the full activation of *rprA* expression in Ea1189Δ*rcsB*(prcsB-D56E) but loss of *rprA* expression in Ea1189Δ*rcsB*(prcsB-K154Q). We also examined *rprA* expression levels in *E. amylovora* cultures under conditions that are known to strongly activate *rprA* expression in *S. enterica* serovar Typhimurium or *E. coli*, including low pH stress, osmotic shock, and high population density (Madhugiri et al., 2010; Srikumar et al., 2015). None of these conditions significantly altered *rprA* expression in *E. amylovora*.

Nevertheless, we found that *rprA* expression was strongly stimulated in *E. amylovora* cultures grown in HrpMM medium, a low nutrient and low pH medium that mimics the plant apoplast (Huynh et al., 1989), and was induced to a greater extent during infection of immature pears. Of note, we also observed differential expression of several virulence factor genes in *E. amylovora* cells from ooze that emerged from the inoculated immature pears in the same direction as in *E. amylovora* cells overexpressing *rprA* in vitro, suggesting the critical roles of RprA during *E. amylovora* pathogenesis on immature pears. Thus, although *E. amylovora*, *E. coli*, and *S. enterica* serovar Typhimurium are all phylogenetically closely related members of the *Enterobacteriaceae* family, *rprA* regulation responds to different environmental cues and is probably optimized for the regulation of specific virulence traits in each of these organisms.

The final stage of biofilm development is dispersal, which allows subpopulations of cells to be detached from the biofilm and resume the planktonic mode of growth (Koczan et al., 2011; Rumbaugh & Sauer, 2020). Although biofilm dispersal in *E. amylovora*, to the best of our knowledge, has not been previously genetically or phenotypically characterized, dispersal is evidently an important step in *E. amylovora* pathogenesis from several lines of evidence: First, *E. amylovora* is capable of migrating systemically within host xylem (Thomson, 2000), which clearly requires cells in the sessile mode of growth to switch back to the planktonic mode of growth to move to new infection sites. Using scanning electron microscopy analyses of longitudinal sections of the central vein of infected apple leaves, we previously visualized the discontinuous aggregation of *E. amylovora* microcolonies (Koczan et al., 2011), suggesting that a cycle of dispersal and re-establishment of biofilms contributes to the systemic movement of *E. amylovora* in apple leaf xylem. In addition, masses of *E. amylovora* cells have been demonstrated to break out of xylem vessels to reach the surrounding intercellular spaces of the cortical

parenchyma cells (Bogs et al., 1998), which is a further example of dispersal from the biofilm and transitioning back to T3SS-mediated pathogenesis.

Our evidence suggests that RprA activates biofilm dispersal in *E. amylovora* and regulates several virulence traits associated with a transition from biofilm development to T3SS-mediated pathogenesis. The induction of motility has been observed during biofilm dispersal in bacteria such as *E. coli* and *Pseudomonas aeruginosa* (Jackson et al., 2002; Purevdorj-Gage et al., 2005; Sauer et al., 2002), and we found that motility is also positively regulated by RprA in *E. amylovora*. Cellulose and levan are important EPS constituents of the biofilm matrix of *E. amylovora* (Castiblanco & Sundin, 2018; Koczan et al., 2009), thus RprA-mediated down-regulation of both cellulose and levan production also suggests a cellular transition away from biofilm development. In contrast to the reduction in cellulose and levan we observed when *rprA* was overexpressed in *E. amylovora* Ea1189, amylovoran production was significantly increased (Figure 2a). This seemingly paradoxical observation can be resolved by the knowledge that amylovoran is a pathogenicity factor in *E. amylovora* (Bellemann & Geider, 1992), and this further indicates that amylovoran production of peripheral cells that are dispersing from biofilms may not be at the level necessary for continuing planktonic stage T3SS-mediated pathogenesis.

In summary, we demonstrated that the Hfq-dependent sRNA RprA exhibits important regulatory roles in orchestrating virulence factors of *E. amylovora* and affects transcriptional or posttranscriptional activity of the virulence factor genes. We showed that *rprA* is maintained at a very low basal level in a rich medium and can be activated by RcsB phosphorylation and by the host apoplast environment. Finally, we provided evidence that RprA plays an important role in the dispersal of *E. amylovora* cells from biofilms. This study sheds light on future mechanistic research into this important biological process during pathogenesis that has not yet been characterized in most phytopathogenic bacteria.

4 | EXPERIMENTAL PROCEDURES

4.1 | Bacterial strains, plasmids, and media

The *E. amylovora* strains, plasmids, and oligonucleotide primers used in this study are listed in Table 1. All strains were routinely maintained in 15% glycerol at −80 °C. Single colonies were grown overnight in LB broth at 28 °C with shaking at 200 rpm for 20 hr. The following antibiotics were amended to media as needed: ampicillin

TABLE 1 Bacteria strains or plasmids used in this study

	Strain or plasmid	Genotype	Reference
Strains	Ea1189	Wild type	Yu et al. (2020)
	Ea1189Δ*rprA*	*rprA* deletion mutant, Cm[R]	Zeng et al. (2013)
	Ea1189Δ*rcsB*	*rcsB* deletion mutant, Cm[R]	Wang et al. (2009)
Plasmids	pBBR1MCS5	Broad-host-range cloning vector, Gm[R]	Kovach et al. (1995)
	pJP-*rprA*	A region spanning the *rprA* gene and its corresponding native promoter in pBBR1MCS-5; Gm[R]	This study
	p*rcsB*	A region spanning the *rcsBD* operon along with its native promoter region in pBBR1MCS5; Gm[R]	This study
	p*rcsB*-D56E	p*rcsB* with an allele change resulting in the amino acid substitution of aspartic acid to glutamic acid at codon 56 in RcsB	This study
	p*rcsB*-K154Q	p*rcsB* with an allele change resulting in the amino acid substitution of lysine to glutamine at codon 154 in RcsB	This study
	pHM-*tac*	IPTG-inducible sRNA overexpression vector, Ap[R]	Park et al. (2013)
	pOE-*rprA*	pHM-*tac*::*rprA*; overexpression vector; Ap[R]	This study
	pPROBE-NT	Broad-host-range promoter-probe vector; Km[R]	Miller et al. (2000)
	pPROBE-*hrpS*	pPROBE-NT::*hrpS*; native promoter of *hrpS* in pPROBE-NT; Km[R]	This study
	pPROBE-*hrpL*	pPROBE-NT::*hrpL*; native promoter of *hrpL* in pPROBE-NT; Km[R]	This study
	pPROBE-*hrpA*	pPROBE-NT::*hrpA*; native promoter of *hrpA* in pPROBE-NT; Km[R]	This study
	pPROBE-*dspE*	pPROBE-NT::*dspE*; native promoter of *dspE* in pPROBE-NT; Km[R]	This study
	pPROBE-*amsG*	pPROBE-NT::*amsG*; native promoter of *amsG* in pPROBE-NT; Km[R]	This study
	pPROBE-*lsc*	pPROBE-NT::*lsc*; native promoter of *lsc* in pPROBE-NT; Km[R]	This study
	pxg-20	Broad-host-range translational fusion vector; Cm[R]	Urban & Vogel (2007)
	pxg-20:*hrpS*129	5′ UTR (129 nt) of *hrpS* and 90 nt into the coding region of *hrpS* in pxg-20; Cm[R]	This study
	pxg-20:*hrpS*227	5′ UTR (227 nt) of *hrpS* and 90 nt into the coding region of *hrpS* in pxg-20; Cm[R]	This study

(100 µg/ml), chloramphenicol (30 µg/ml), gentamicin (15 µg/ml), and kanamycin (50 µg/ml).

4.2 | DNA manipulations

To generate the pJP-*rprA* construct for *rprA* complementation, the *rprA* gene along with its native promoter region was cloned into the low-copy plasmid pBBR1MCS5. To generate the *rprA* overexpression construct, the *rprA* full-length gene sequence was cloned into pHM-*tac* immediate downstream of the isopropyl β-D-1-thiogalactopyranoside (IPTG)-inducible *tac* promoter. To generate the construct p*rcsBD* for *rcsB* complementation, the *rcsBD* operon along with its native promoter region was cloned into pBBR1MCS5. The p*rcsB*-D56E and p*rcsB*-K154Q constructs, which allow expression of *rcsB* with a D56E substitution or a K154Q substitution, respectively, were generated through site-directed mutagenesis using the QuikChange Lightning kit. To generate the transcriptional fusion constructs, including pPROBE-NT:*hrpL*, pPROBE-NT:*hrpA*, pPROBE-NT:*dspE*, pPROBE-NT:*amsG*, and pPROBE-NT:*lsc*, the promoter region of the corresponding genes (c.500-bp amplicons upstream of the start codon) were cloned immediately upstream of the promoter-less *gfp* gene in pPROBE-NT (Miller et al., 2000). To generate the translation fusion constructs pxg-20:*hrpS*129 and pxg-20:*hrpS*227, the 5′ UTR regions of *hrpS* were amplified from the two transcriptional start sites to 90 nt into the coding region and were cloned in-frame with *gfp* in pXG-20 (Urban & Vogel, 2007). The transcription start sites of *hrpS* were identified previously (Lee & Zhao, 2018). To generate p*NptII-gfp-rprA-mCherry*, the *Dickeya dadantii hrpA* promoter region in *nptII-gfp-hrpA-mCherry* (Cui et al., 2018) was replaced with the promoter region of *E. amylovora rprA*. Constructs were cloned using the standard ligation-dependent approach (Sambrook, 2001) or a ligation-independent cloning approach (Li et al., 2011). The strains or plasmids used in this study are listed in Table 1. The oligonucleotide primers used are listed in Table 2. Constructs were transformed into *E. coli* Turbo cells using transformation and storage solution (TSS) (Chung et al., 1989) and/or into *E. amylovora* through electroporation.

4.3 | Bioinformatics

The secondary structure of RprA was predicted using the minimum free energy model of RNAfold (http://rna.tbi.univie.ac.at/cgi-bin/RNAWebSuite/RNAfold.cgi). The genome-wide targets of RprA were predicted using TargetRNA2 (http://cs.wellesley.edu/~btjaden/TargetRNA2/) with the default setting.

4.4 | Quantification of amylovoran

The concentration of amylovoran was determined through a turbidity-based assay using cetylpyrimidinium chloride (CPC) with modifications (Bellemann et al., 1994). Briefly, overnight *E. amylovora* cultures grown in LB medium were washed twice and resuspended in modified basal medium A (MBMA; Edmunds et al., 2013) supplemented with 1% galactose. Cultures were grown for 24 hr at 28 °C with shaking at 200 rpm. After centrifugation at $16,000 \times g$ for 2 min, supernatant was harvested and mixed with 50 µl of 50 mg/ml CPC (Sigma-Aldrich) per millilitre of culture supernatant. The mixtures were incubated at room temperature for 5 min and their turbidity at OD_{600} was measured using a spectrophotometer (Tecan) followed by normalization with the OD_{600} of the cultures.

4.5 | Swimming motility assay

Swimming motility was examined following the method of Edmunds et al. (2013) with modifications. Briefly, 2 µl of overnight *E. amylovora* culture was stab-inoculated into 0.3% agar LB plates and the inoculated plates were inoculated at 28 °C for 48 hr without any agitation. The radius of the motility area was determined for the subsequent statistical analysis.

4.6 | Cellulose assay

Cellulose biosynthesis was assessed following a previously described method (Castiblanco & Sundin, 2018). In brief, 5 µl of *E. amylovora* overnight culture was spotted on NaCl-free LB plates supplemented with Congo red (40 µg/ml). The inoculated plates were incubated for 48 hr at 28 °C without shaking. Red coloration of the *E. amylovora* colony is indicative of the production of cellulose that binds to Congo red.

4.7 | Levansucrase activity

Levansucrase activity was quantified as described previously (Schachterle & Sundin, 2019). In brief, supernatants of *E. amylovora* overnight cultures were mixed with $0.5 \times$ phosphate-buffered saline (PBS) containing 2 M sucrose in a 1:1 ratio. The mixtures were incubated at 37 °C for 4 hr without shaking. The resultant turbidity from levan production, which is catalysed by the levansucrase enzyme, was measured at OD_{600} using a spectrophotometer (Tecan) followed by normalization with the OD_{600} values of the cultures.

4.8 | Hypersensitive response assay

The HR assay followed the protocol of Zeng and Sundin (2014). In brief, overnight *E. amylovora* cultures were harvested, washed, and adjusted to the optical density $OD_{600} = 0.05$ in $0.5 \times$ PBS. Around 100 µl cell suspension was infiltrated into *N. benthamiana* leaves of 10-week-old plants with a needleless syringe. The HR symptom was observed and image-captured 16 hr postinfiltration.

TABLE 2 Oligonucleotide primers used in this study

Primer name	Sequence (5′-3′)	Purpose
com_rprAF	TAGGAATTCGCAATAATCTGGCTTTACTGGA	Primers used for *rprA* complementation
com_rprAR	ATATCTAGATCGGTTCACCGATCGTCC	
oe_rprAF	GACGAATTCAGGATTTGAAATCTTCCCACTGA	Primer used for *rprA* overexpression
oe_rprAR	GACTCTAGACCGATCGTCCTTTTTTAAGGGC	
com_RcsBD_F	CCCGACTGGAAAGCGGGCAGTGCTAGCACAATTCACAAGGTTGG	Primer used for *rcsB* complementation
com_RcsBD_R	GTTGCGTCGCGGTGCATGGCTCCTAATGAACTGCCGCTACT	
backbone_pBBR1MCS5_F	CACTGCCCGCTTTCCAGTCGGG	
backbone_pBBR1MCS5_R	CCATGCACCGCGACGCAAC	
RcsB_D56E_F	CCAGGCATCGAAAGCTCGGTGACCAGCAC	Primers used for site-directed mutagenesis of p*rcsB*
RcsB_D56E_R	GTGCTGGTCACCGAGCTTTCGATGCCTGG	
RcsB_K154Q_F	GCGCAGAACTTCGCTCTCCTGCGGTGACAAACGCTTATC	
RcsB_K154Q_R	GATAAGCGTTTGTCACCGCAGGAGAGCGAAGTTCTGCGC	
hrpS_tsc_F	CGACCTGAATGGAAGCCGGCAGATTGTCTTTGCCGAGTACA	Primers used for transcriptional fusion constructions
hrpS_tsc_R	GAGCTCGGTACCCGGGGATCCTCAAAAAATTACCCCTGCCCTATC	
tsc_hrpL_F	CGACCTGAATGGAAGCCGGCTAAACGCGCATGCTGCGGAT	
tsc_hrpL_R	GAGCTCGGTACCCGGGGATCCTCGGCTTGCTCCGTTACTAAATCA	
tsc_dspE_F	CGACCTGAATGGAAGCCGGCCTGACTGTCAGACTGCGGAGTGG	
tsc_dspE_R	GAGCTCGGTACCCGGGGATCCTCGACCCGTTGCCCCCACCCTCT	
tsc_hrpA_F	CGACCTGAATGGAAGCCGGCCTGGTGAAGGCGCACCGGGAT	
tsc_hrpA_R	GAGCTCGGTACCCGGGGATCCTCATTAATCTCTCCAATTATTGAGGTTGTGTTCC	
tsc_lsc_F	CGACCTGAATGGAAGCCGGCAAGTGCACCTCCGCAAGGT	
tsc_lsc_R	GAGCTCGGTACCCGGGGATCCTC AAATATCCTCACAGGTTATTTCG	
backbone_pPROBE-NT_F	GAGGATCCCCGGGTACCGAGCTC	
backbone_pPROBE-NT_R	GCCGGCTTCCATTCAGGTCG	
tsc_amsG_F	CGACCTGAATGGAAGCCGGCCCTTAATGAGATGGTTGATAAATCCAT	
tsc_amsG_R	GAGCTCGGTACCCGGGGATCCTCAATTAGCTCTTAATTTTATCTCAGG	
tln_dspE_F	GAGATTGACATCCCTATCAGTGATAGAGATACTGAGCACAAAAATATCTAATGTTTACGGCAGAGG	Primers used for translational fusion constructs
tln_dspE_R	AGTTCTTCTCCTTTGCTCATGAATTCGCCAGAACCCTGCTGTAAGGCAACACC	
tln_hrpS129_F	GAGATTGACATCCCTATCAGTGATAGAGATACTGAGCACACAGCGTAAACTCAGAGTAAATA	
tln_hrpS227_F	GAGATTGACATCCCTATCAGTGATAGAGATACTGAGCACAATGTAGGGTAATCCCTACATTGC	
tln_hrpS_R	AGTTCTTCTCCTTTGCTCATGAATTCGCCAGAACCGATATCGATGGGTTGTTCTTCTGT	
backbone_pxg20_F	GAAGGTTCTGGCGAATTCATGAGCAAAGGAGAAGAACT	
backbone_pxg20_R	TGTGCTCAGTATCTCTATCACTGATAGGGATGTCAATCTC	
NptII-gfp-rprA-mCherry_F	GTTGGATCCGCAATAATCTGGCTTTACTG	Primers used for generating p*NptII-gfp-rprA-mCherry*
NptII-gfp-rprA-mCherry_R	GGTGAGCTCGTAACCATAGTATGAAAAGGTG	

4.9 | Confocal microscopy

A FluoView 1000 (Olympus) laser scanning confocal microscope was used for examining *E. amylovora* cells expressing the *nptII-gfp-rprA-mCherry* construct, which expressed gfp in a constitutive manner and mCherry under the control of the native promoter of *rprA*. To analyse *rprA* promoter activity in vitro, overnight cultures of *E. amylovora* Ea1189(*nptII-gfp-rprA-mCherry*) were washed and resuspended in fresh LB medium with the OD_{600} adjusted to 1.0. To measure in vivo *rprA* promoter activity in pear ooze or pear flesh, *E. amylovora* Ea1189(*nptII-gfp-rprA-mCherry*) cultures were inoculated on immature pears as described previously (Edmunds et al., 2013), except that the starting amount of inoculum was approximately 2×10^5 cfu to accelerate the infection and ooze emergence. Pear ooze was harvested using a sterile inoculation loop and was resuspended in $0.5 \times$ PBS to $OD_{600} = 1.0$ immediately before imaging. Infected pear flesh tissue was dissected using a sterile razor blade immediately before imaging.

The laser at 488 nm and the SDM560-BA505-525 emission filter were used for capturing the gfp fluorescence. The laser at 561 nm and the SDM640-BA560-620 emission filter were used for capturing the mCherry fluorescence. A sequential imaging recording method was used to avoid crosstalk between the fluorochromes.

4.10 | Total RNA extraction and RT-qPCR

Overnight *E. amylovora* cultures were washed and diluted to $OD_{600} = 0.05$ in fresh LB broth. The cultures were grown at 28 °C with shaking until the optical density reached $OD_{600} = 0.5$, corresponding to the exponential stage of bacterial growth. To examine the effect of environmental stressors on *rprA* expression, cultures of *E. amylovora* Ea1189 at $OD_{600} = 0.5$ were washed and resuspended in the same volume of the following media for 2 hr: LB medium, LB medium (pH 5.1), LB medium amended 0.4 M NaCl, and HrpMM (Huynh et al., 1989). To examine the effect of growth stage on *rprA* expression, late stationary phase cultures of *E. amylovora* were prepared by allowing cultures in the exponential phase to continue to grow for another 16 hr. To compare the in vivo and the in vitro expression of *rprA* and virulence factor genes in *E. amylovora*, *E. amylovora* Ea1189 was either inoculated into immature pears or grown overnight following the same procedures used for the confocal microscopic studies. To obtain enough *E. amylovora* cells from pear ooze and also to control the possible variations of *E. amylovora* gene expression due to the physiological differences of the pears inoculated, ooze from six inoculated pears was pooled together as one biological replicate and three biological replicates were investigated in this study, "Ooze 1", "Ooze 2", and "Ooze 3." Crude total RNA was extracted following a previously reported method (Rivas et al., 2001). Crude total RNA was purified using the RNA Clean & Concentrator-25 kit (Zymo Research) following the manufacturer's instructions. Contaminating genomic DNA was eliminated using the TURBO DNA-free kit (Thermo Fisher Scientific) according to the manufacturer's instructions. First-strand cDNA was synthesized with the High Capacity cDNA Reverse Transcription kit (Thermo Fisher Scientific) according to the manufacturer's instructions. Expression levels of RprA were quantified routinely using a StepOne Plus Real-Time PCR system (Applied Biosystems) (Zeng et al., 2013). The reference gene *recA* was used as an endogenous control (Zeng et al., 2013). Relative expression values were calculated through the $2^{-\Delta\Delta Ct}$ method.

4.11 | Biofilm assay

Overnight cultures of *E. amylovora* Ea1189(pHM-*tac*) and Ea1189(pOE-*rprA*) were washed and resuspended in $0.5 \times$ LB medium with the OD_{600} adjusted to 1.0. To enhance attachment of *E. amylovora* cells, wells of 96-well round-bottom microplates were etched with 200 μl acetone for 20 s to increase the roughness of the surface (Davies & Marques, 2009). After complete drying of the plates, resuspended *E. amylovora* cultures in 200 μl per well were inoculated and incubated at room temperature for 48 hr with light horizontal shaking. After depletion of planktonic cultures, biofilm cells were stained by adding 250 μl of 10% crystal violet solution for 1 hr. Stained plates were washed twice by water and dried. A total of 300 μl of destaining solution (40% methanol and 10% acetic acid) was added into each well incubated for 1 hr at room temperature with light shaking. The A_{594} values of the suspensions were measured using a Tecan spectrophotometer.

4.12 | Biofilm dispersal assay

Two millilitres of washed overnight cultures at OD_{600} of 1 in $0.5 \times$ LB medium were inoculated into 12-well plates without adding any IPTG. One polystyrene bead (7 mm) was added to each inoculated well. The inoculated plates were incubated at room temperature for 48 hr with light shaking to allow even formation of biofilms on the beads. Each bead covered with biofilm cells was washed six times by 10 ml of $0.5 \times$ PBS to remove any planktonic cells on the surface of the bead. Washed beads were transferred to wells in 2 ml of fresh $0.5 \times$ LB medium and 1 mM IPTG and incubated at room temperature without any shaking. Dispersed cells were quantified by withdrawing 10 μl of the culture suspension at 1-hr intervals, and the cfus were determined by dilution plating. To count the starting number of biofilm cells on the beads, beads with biofilm cells attached were added into 1.7-ml Eppendorf centrifuge tubes containing 1 ml of $0.5 \times$ PBS followed by sonication for 5 min to release the attached cells. The cfus of the suspension were counted through dilution plating.

4.13 | Statistical analyses

Results represent the means of at least three replications, and error bars represent the standard deviations. Statistical analyses of Student's *t* test or Tukey's HSD test were performed using JMP Pro 14 statistical software.

AUTHOR CONTRIBUTIONS

J.P., J.K.S., and G.W.S. designed the experiments. J.P. and J.K.S. performed the experiments. J.P. and G.W.S. wrote the manuscript. All authors contributed to the revisions.

DATA AVAILABILITY STATEMENT

The data that support the findings of this study are available from the corresponding author upon reasonable request.

ORCID

George W. Sundin ![iD] https://orcid.org/0000-0003-4078-8368

REFERENCES

Ancona, V., Chatnaparat, T. & Zhao, Y. (2015) Conserved aspartate and lysine residues of RcsB are required for amylovoran biosynthesis, virulence, and DNA binding in *Erwinia amylovora*. *Molecular Genetics and Genomics*, 290, 1265–1276.

Andreassen, P.R., Pettersen, J.S., Szczerba, M., Valentin-Hansen, P., Møller-Jensen, J. & Jørgensen, M.G. (2018) sRNA-dependent control of curli biosynthesis in *Escherichia coli*: McaS directs endonucleolytic cleavage of *csgD* mRNA. *Nucleic Acids Research*, 46, 6746–6760.

Bayot, R.G. & Ries, S.M. (1986) Role of motility in apple blossom infection by *Erwinia amylovora* and studies of fire blight control with attractant and repellent compounds. *Phytopathology*, 76, 441–445.

Bellemann, P., Bereswill, S., Berger, S. & Geider, K. (1994) Visualization of capsule formation by *Erwinia amylovora* and assays to determine amylovoran synthesis. *International Journal of Biological Macromolecules*, 16, 290–296.

Bellemann, P. & Geider, K. (1992) Localization of transposon insertions in pathogenicity mutants of *Erwinia amylovora* and their biochemical characterization. *Microbiology*, 138, 931–940.

Bogdanove, A.J., Bauer, D.W. & Beer, S.V. (1998) *Erwinia amylovora* secretes DspE, a pathogenicity factor and functional AvrE homolog, through the Hrp (type III secretion) pathway. *Journal of Bacteriology*, 180, 2244–2247.

Bogs, J., Bruchmüller, I., Erbar, C. & Geider, K. (1998) Colonization of host plants by the fire blight pathogen *Erwinia amylovora* marked with genes for bioluminescence and fluorescence. *Phytopathology*, 88, 416–421.

Brennan, R.G. & Link, T.M. (2007) Hfq structure, function and ligand binding. *Current Opinion in Microbiology*, 10, 125–133.

Bugert, P. & Geider, K. (1995) Molecular analysis of the *ams* operon required for exopolysaccharide synthesis of *Erwinia amylovora*. *Molecular Microbiology*, 15, 917–933.

Castiblanco, L.F. & Sundin, G.W. (2016) New insights on molecular regulation of biofilm formation in plant-associated bacteria. *Journal of Integrative Plant Biology*, 58, 362–372.

Castiblanco, L.F. & Sundin, G.W. (2018) Cellulose production, activated by cyclic di-GMP through BcsA and BcsZ, is a virulence factor and an essential determinant of the three-dimensional architectures of biofilms formed by *Erwinia amylovora* Ea1189. *Molecular Plant Pathology*, 19, 90–103.

Chung, C.T., Niemela, S.L. & Miller, R.H. (1989) One-step preparation of competent *Escherichia coli*: transformation and storage of bacterial cells in the same solution. *Proceedings of the National Academy of Sciences of the United States of America*, 86, 2172–2175.

Cui, Z., Yuan, X., Yang, C.H., Huntley, R.B., Sun, W., Wang, J. et al. (2018) Development of a method to monitor gene expression in single bacterial cells during the interaction with plants and use to study the expression of the type III secretion system in single cells of *Dickeya dadantii* in potato. *Frontiers in Microbiology*, 9, 1429.

Davies, D.G. & Marques, C.N. (2009) A fatty acid messenger is responsible for inducing dispersion in microbial biofilms. *Journal of Bacteriology*, 191, 1393–1403.

Edmunds, A.C., Castiblanco, L.F., Sundin, G.W. & Waters, C.M. (2013) Cyclic Di-GMP modulates the disease progression of *Erwinia amylovora*. *Journal of Bacteriology*, 195, 2155–2165.

Geier, G. & Geider, K. (1993) Characterization and influence on virulence of the levansucrase gene from the fireblight pathogen *Erwinia amylovora*. *Physiological and Molecular Plant Pathology*, 42, 387–404.

Goodman, R.N., Huang, J.S. & Huang, P.-Y. (1974) Host-specific phytotoxic polysaccharide from apple tissue infected by *Erwinia amylovora*. *Science*, 183, 1081–1082.

Gross, M., Geier, G., Rudolph, K. & Geider, K. (1992) Levan and levansucrase synthesized by the fireblight pathogen *Erwinia amylovora*. *Physiological and Molecular Plant Pathology*, 40, 371–381.

Hu, L.I., Chi, B.K., Kuhn, M.L., Filippova, E.V., Walker-Peddakotla, A.J., Bäsell, K. et al. (2013) Acetylation of the response regulator RcsB controls transcription from a small RNA promoter. *Journal of Bacteriology*, 195, 4174–4186.

Huang, Y.H., Ferrières, L. & Clarke, D.J. (2006) The role of the Rcs phosphorelay in Enterobacteriaceae. *Research in Microbiology*, 157, 206–212.

Huynh, T.V., Dahlbeck, D. & Staskawicz, B.J. (1989) Bacterial blight of soybean: regulation of a pathogen gene determining host cultivar specificity. *Science*, 245, 1374–1377.

Jackson, D.W., Suzuki, K., Oakford, L., Simecka, J.W., Hart, M.E. & Romeo, T. (2002) Biofilm formation and dispersal under the influence of the global regulator CsrA of *Escherichia coli*. *Journal of Bacteriology*, 184, 290–301.

Kery, M.B., Feldman, M., Livny, J. & Tjaden, B. (2014) TargetRNA2: identifying targets of small regulatory RNAs in bacteria. *Nucleic Acids Research*, 42, W124–W129.

Kharadi, R.R. & Sundin, G.W. (2020) Dissecting the process of xylem colonization through biofilm formation in *Erwinia amylovora*. *Journal of Plant Pathology*. https://doi.org/10.1007/s42161-020-00635-x

Kim, J., Mannaa, M., Kim, N., Lee, C., Kim, J., Park, J. et al. (2018) The roles of two *hfq* genes in the virulence and stress resistance of *Burkholderia glumae*. *The Plant Pathology Journal*, 34, 412.

Kim, J.F., Wei, Z.M. & Beer, S.V. (1997) The *hrpA* and *hrpC* operons of *Erwinia amylovora* encode components of a type III pathway that secretes harpin. *Journal of Bacteriology*, 179, 1690–1697.

Koczan, J.M., Lenneman, B.R., McGrath, M.J. & Sundin, G.W. (2011) Cell surface attachment structures contribute to biofilm formation and xylem colonization by *Erwinia amylovora*. *Applied and Environmental Microbiology*, 77, 7031–7039.

Koczan, J.M., McGrath, M.J., Zhao, Y. & Sundin, G.W. (2009) Contribution of *Erwinia amylovora* exopolysaccharides amylovoran and levan to biofilm formation: implications in pathogenicity. *Phytopathology*, 99, 1237–1244.

Kovach, M.E., Elzer, P.H., Hill, D.S., Robertson, G.T., Farris, M.A., Roop, R.M. 2nd et al. (1995) Four new derivatives of the broad-host-range cloning vector pBBR1MCS, carrying different antibiotic-resistance cassettes. *Gene*, 166, 175–176.

Lai, J.-L., Tang, D.-J., Liang, Y.-W., Zhang, R., Chen, Q., Qin, Z.-P. et al. (2018) The RNA chaperone Hfq is important for the virulence, motility and stress tolerance in the phytopathogen *Xanthomonas campestris*. *Environmental Microbiology Reports*, 10, 542–554.

Lee, J.H., Sundin, G.W. & Zhao, Y. (2016) Identification of the HrpS binding site in the *hrpL* promoter and effect of the RpoN binding site of HrpS on the regulation of the type III secretion system in *Erwinia amylovora*. *Molecular Plant Pathology*, 17, 691–702.

Lee, J.H. & Zhao, Y. (2018) Integration of multiple stimuli-sensing systems to regulate HrpS and type III secretion system in *Erwinia amylovora*. *Molecular Genetics and Genomics*, 293, 187–196.

Li, C., Wen, A., Shen, B., Lu, J., Huang, Y. & Chang, Y. (2011) FastCloning: a highly simplified, purification-free, sequence- and ligation-independent PCR cloning method. *BMC Biotechnology*, 11, 92.

Madhugiri, R., Basineni, S.R. & Klug, G. (2010) Turn-over of the small non-coding RNA RprA in *E. coli* is influenced by osmolarity. *Molecular Genetics and Genomics*, 284, 307–318.

Majdalani, N., Chen, S., Murrow, J., St John, K. & Gottesman, S. (2001) Regulation of RpoS by a novel small RNA: the characterization of RprA. *Molecular Microbiology*, 39, 1382–1394.

Majdalani, N., Heck, M., Stout, V. & Gottesman, S. (2005) Role of RcsF in signaling to the Rcs phosphorelay pathway in *Escherichia coli*. *Journal of Bacteriology*, 187, 6770–6778.

Majdalani, N., Hernandez, D. & Gottesman, S. (2002) Regulation and mode of action of the second small RNA activator of RpoS translation, RprA. *Molecular Microbiology*, 46, 813–826.

Malnoy, M., Martens, S., Norelli, J.L., Barny, M.A., Sundin, G.W., Smits, T.H. et al. (2012) Fire blight: applied genomic insights of the pathogen and host. *Annual Review of Phytopathology*, 50, 475–494.

McCullen, C.A., Benhammou, J.N., Majdalani, N. & Gottesman, S. (2010) Mechanism of positive regulation by DsrA and RprA small noncoding RNAs: pairing increases translation and protects mRNA from degradation. *Journal of Bacteriology*, 192, 5559.

McNally, R.R., Toth, I.K., Cock, P.J., Pritchard, L., Hedley, P.E., Morris, J.A. et al. (2012) Genetic characterization of the HrpL regulon of the fire blight pathogen *Erwinia amylovora* reveals novel virulence factors. *Molecular Plant Pathology*, 13, 160–173.

Mika, F., Busse, S., Possling, A., Berkholz, J., Tschowri, N., Sommerfeldt, N. et al. (2012) Targeting of *csgD* by the small regulatory RNA RprA links stationary phase, biofilm formation and cell envelope stress in *Escherichia coli*. *Molecular Microbiology*, 84, 51–65.

Miller, W.G., Leveau, J.H. & Lindow, S.E. (2000) Improved *gfp* and *inaZ* broad-host-range promoter-probe vectors. *Molecular Plant-Microbe Interactions*, 13, 1243–1250.

Mina, I.R., Jana, N.P., Criollo, J.E. & Castiollo, J.A. (2019) The critical role of biofilms in bacterial vascular plant pathogenesis. *Plant Pathology*, 68, 1439–1447.

Nimtz, M., Mort, A., Domke, T., Wray, V., Zhang, Y., Qiu, F. et al. (1996) Structure of amylovoran, the capsular exopolysaccharide from the fire blight pathogen *Erwinia amylovora*. *Carbohydrate Research*, 287, 59–76.

Norelli, J.L., Jones, A.L. & Aldwinckle, H.S. (2003) Fire blight management in the twenty-first century: using new technologies that enhance host resistance in apple. *Plant Disease*, 87, 756–765.

Oh, C.S., Kim, J.F. & Beer, S.V. (2005) The Hrp pathogenicity island of *Erwinia amylovora* and identification of three novel genes required for systemic infection. *Molecular Plant Pathology*, 6, 125–138.

Park, H., Bak, G., Kim, S.C. & Lee, Y. (2013) Exploring sRNA-mediated gene silencing mechanisms using artificial small RNAs derived from a natural RNA scaffold in *Escherichia coli*. *Nucleic Acids Research*, 41, 3787–3804.

Purevdorj-Gage, B., Costerton, W.J. & Stoodley, P. (2005) Phenotypic differentiation and seeding dispersal in non-mucoid and mucoid *Pseudomonas aeruginosa* biofilms. *Microbiology*, 151, 1569–1576.

Rivas, R., Vizcaíno, N., Buey, R.M., Mateos, P.F., Martínez-Molina, E. & Velázquez, E. (2001) An effective, rapid and simple method for total RNA extraction from bacteria and yeast. *Journal of Microbiological Methods*, 47, 59–63.

Rumbaugh, K.P. & Sauer, K. (2020) Biofilm dispersion. *Nature Reviews Microbiology*, 18, 571–586.

Sambrook, J. (2001) *Molecular cloning: a laboratory manual.* 3rd edition. Cold Spring Harbor, NY: Cold Spring Harbor Laboratory Press.

Sauer, K., Camper, A.K., Ehrlich, G.D., Costerton, J.W. & Davies, D.G. (2002) *Pseudomonas aeruginosa* displays multiple phenotypes during development as a biofilm. *Journal of Bacteriology*, 184, 1140–1154.

Schachterle, J.K. & Sundin, G.W. (2019) The leucine-responsive regulatory protein Lrp participates in virulence regulation downstream of small RNA ArcZ in *Erwinia amylovora*. *mBio*, 10, e00757-19.

Schachterle, J.S., Zeng, Q. & Sundin, G.W. (2019) Three Hfq-dependent small RNAs regulate flagellar motility in the fire blight pathogen *Erwinia amylovora*. *Molecular Microbiology*, 111, 1476–1492.

Sjulin, T.M. & Beer, S.V. (1978) Mechanism of wilt induction by amylovorin in cotoneaster shoots and Its relation to wilting of shoots infected by *Erwinia amylovora*. *Phytopathology*, 68, 89–94.

Slack, S.M., Zeng, Q., Outwater, C.A. & Sundin, G.W. (2017) Microbiological examination of *Erwinia amylovora* exopolysaccharide ooze. *Phytopathology*, 107, 403–411.

Srikumar, S., Kröger, C., Hébrard, M., Colgan, A., Owen, S.V., Sivasankaran, S.K. et al. (2015) RNA-seq brings new insights to the intra-macrophage transcriptome of *Salmonella Typhimurium*. *PLoS Pathogens*, 11, e1005262.

Szczesny, M., Beloin, C. & Ghigo, J.M. (2018) Increased osmolarity in biofilm triggers RcsB-dependent lipid A palmitoylation in *Escherichia coli*. *mBio*, 9, e01415-18.

Thomson, S.V. (2000) Epidemiology of fire blight. In: Vanneste, J. (Ed.) *Fire blight: the disease and its causative agent, Erwinia amylovora*. New York: CABI Publishing, pp. 9–36.

Triplett, L.R., Melotto, M. & Sundin, G.W. (2009) Functional analysis of the N terminus of the *Erwinia amylovora* secreted effector DspA/E reveals features required for secretion, translocation, and binding to the chaperone DspB/F. *Molecular Plant-Microbe Interactions*, 22, 1282–1292.

Urban, J.H. & Vogel, J. (2007) Translational control and target recognition by *Escherichia coli* small RNAs *in vivo*. *Nucleic Acids Research*, 35, 1018–1037.

Vanneste, J.L. (1995) *Erwinia amylovora*. In: Singh, U.S., Singh, R.P., & Kohmoto, K. (Eds.) *Pathogenesis and host specificity in plant diseases: histopathological, biochemical, genetic and molecular bases*, 21–46. Oxford and London: Pergammon Press.

Vogel, J. & Luisi, B.F. (2011) Hfq and its constellation of RNA. *Nature Reviews Microbiology*, 9, 578–589.

Wang, C., Pu, T., Lou, W., Wang, Y., Gao, Z., Hu, B. et al. (2018) Hfq, a RNA chaperone, contributes to virulence by regulating plant cell wall–degrading enzyme production, type VI secretion system expression, bacterial competition, and suppressing host defense response in *Pectobacterium carotovorum*. *Molecular Plant-Microbe Interactions*, 31, 1166–1178.

Wang, D., Korban, S.S. & Zhao, Y. (2009) The Rcs phosphorelay system is essential for pathogenicity in *Erwinia amylovora*. *Molecular Plant Pathology*, 10, 277–290.

Wang, D., Korban, S.S., Pusey, P.L. & Zhao, Y. (2012a) AmyR is a novel negative regulator of amylovoran production in *Erwinia amylovora*. *PLoS One*, 7, e45038.

Wang, D., Qi, M., Calla, B., Korban, S.S., Clough, S.J., Cock, P.J.A. et al. (2012b) Genome-wide identification of genes regulated by the Rcs phosphorelay system in *Erwinia amylovora*. *Molecular Plant-Microbe Interactions*, 25, 6–17.

Wei, Z.M. & Beer, S.V. (1995) *hrpL* activates *Erwinia amylovora hrp* gene transcription and is a member of the ECF subfamily of sigma factors. *Journal of Bacteriology*, 177, 6201–6210.

Wei, Z., Kim, J.F. & Beer, S.V. (2000) Regulation of hrp genes and type III protein secretion in *Erwinia amylovora* by HrpX/HrpY, a novel two-component system, and HrpS. *Molecular Plant-Microbe Interactions*, 13, 1251–1262.

Wilms, I., Möller, P., Stock, A.-M., Gurski, R., Lai, E.-M. & Narberhaus, F. (2012) Hfq influences multiple transport systems and virulence in the plant pathogen *Agrobacterium tumefaciens*. *Journal of Bacteriology*, 194, 5209–5217.

Yu, M., Singh, J., Khan, A., Sundin, G.W. & Zhao, Y.F. (2020) Complete genome sequence of the fire blight pathogen *Erwinia amylovora* strain Ea1189. *Molecular Plant-Microbe Interactions*, 33, 1277–1279. https://doi.org/10.1094/MPMI-06-20-0158-A.

Yuan, X., Zeng, Q., Khokhani, D., Tian, F., Severin, G.B., Waters, C.M. et al. (2019) A feed-forward signaling circuit controls bacterial virulence through linking cyclic di-GMP and two mechanistically distinct sRNAs, ArcZ and RsmB. *Environmental Microbiology*, 21, 2755–2771.

Zeng, Q., McNally, R.R. & Sundin, G.W. (2013) Global small RNA chaperone Hfq and regulatory small RNAs are important virulence regulators in *Erwinia amylovora*. *Journal of Bacteriology*, 195, 1706–1717.

Zeng, Q. & Sundin, G.W. (2014) Genome-wide identification of Hfq-regulated small RNAs in the fire blight pathogen *Erwinia amylovora* discovered small RNAs with virulence regulatory function. *BMC Genomics*, 15, 414.

Zhao, Y., Sundin, G.W. & Wang, D. (2009a) Construction and analysis of pathogenicity island deletion mutants of *Erwinia amylovora*. *Canadian Journal of Microbiology*, 55, 457–464.

Zhao, Y., Wang, D., Nakka, S., Sundin, G.W. & Korban, S.S. (2009b) Systems level analysis of two-component signal transduction systems in *Erwinia amylovora*: Role in virulence, regulation of amylovoran biosynthesis and swarming motility. *BMC Genomics*, 10, 245.

SUPPORTING INFORMATION

Additional supporting information may be found online in the Supporting Information section.